Original Article

Experimental glaucoma microstent implantation in two animal models and human donor eyes—an *ex vivo* micro-computed tomography-based evaluation of applicability

Jens Runge[1,2]^, Sabine Kischkel[3]^, Jonas Keiler[2]^, Niels Grabow[3], Klaus-Peter Schmitz[3,4], Stefan Siewert[4]^, Andreas Wree[2], Rudolf F. Guthoff[1], Thomas Stahnke[1,4,5]^

[1]Department of Ophthalmology, Rostock University Medical Center, Rostock, Germany; [2]Institute of Anatomy, Rostock University Medical Center, Rostock, Germany; [3]Institute of Biomedical Engineering, Rostock University Medical Center, Rostock, Germany; [4]Institute for Implant Technology and Biomaterials e.V., Rostock-Warnemünde, Germany; [5]Department of Life, Light & Matter, University of Rostock, Rostock, Germany

Contributions: (I) Conception and design: J Runge, J Keiler, KP Schmitz, RF Guthoff, T Stahnke; (II) Administrative support: J Keiler, A Wree, RF Guthoff, T Stahnke; (III) Provision of study materials or patients: S Kischkel, J Keiler, KP Schmitz, N Grabow, S Siewert, T Stahnke; (IV) Collection and assembly of data: J Runge, S Kischkel, N Grabow, S Siewert, RF Guthoff, T Stahnke; (V) Data analysis and interpretation: J Runge, J Keiler, A Wree, T Stahnke; (VI) Manuscript writing: All authors; (VII) Final approval of manuscript: All authors.

Correspondence to: Thomas Stahnke, DSc. Institute for ImplantTechnology and Biomaterials e.V., Friedrich-Barnewitz-Straße 4, 18119 Rostock-Warnemünde, Germany; Department of Ophthalmology, Rostock University Medical Center, Doberaner Straße 140, 18057 Rostock, Germany; Department Life, Light & Matter, University of Rostock, Albert-Einstein-Straße 25, 18059 Rostock, Germany. Email: thomas.stahnke@iib-ev.de.

Background: Minimally invasive glaucoma surgery (MIGS) has become an important treatment approach for primary open angle glaucoma. Restoration of aqueous humour drainage by means of alloplastic implants represents a promising treatment option and is itself subject of methodological development. An adequate positioning in the targeted tissue regions is essential is important for the performance of our in-house developed Rostock glaucoma microstent (RGM). The aim of this study was to evaluate the applicability of two animal models and human donor eyes regarding RGM placement.

Methods: Eyes were obtained from rabbits, pigs, and human body donations. After orbital exenterations, RGMs were placed in the anterior chamber draining in the subconjunctival space. X-ray contrast was increased by incubation in aqueous iodine solution for subsequent detailed micro-computed tomography (micro-CT)-based visualization and analysis.

Results: In contrast to the human and porcine eyes, the stent extended far to the posterior pole with a more pronounced curvature along the globe in the rabbit eyes due to their smaller size. However, dysfunctional deformations were not depicted. Adequate positioning of the stent's inflow area in the anterior chamber and the outflow area in the Tenon space was achieved in both the animal models and the human eye.

Conclusions: Micro-CT has proven to be a valuable tool for postoperative *ex vivo* evaluation of glaucoma drainage devices in its entire complexity. With regard to morphology, the porcine eye is the ideal animal model to test implantation procedures of the RGM. Nevertheless, rabbit eye morphology facilitates successful implantation results and provides all prerequisites for preclinical animal studies.

Keywords: Alloplastic implant; micro-computed tomography (micro-CT); minimally invasive glaucoma surgery (MIGS); Rostock glaucoma microstent (RGM); 3Rs principle

^ ORCID: Jens Runge, 0000-0002-6883-7961; Sabine Kischkel, 0000-0002-5018-3920; Jonas Keiler, 0000-0003-0893-3254; Stefan Siewert, 0000-0002-8139-0471; Thomas Stahnke, 0000-0003-2425-7268.

Submitted Jun 23, 2023. Accepted for publication Nov 20, 2023. Published online Jan 22, 2024.
doi: 10.21037/qims-23-905
View this article at: https://dx.doi.org/10.21037/qims-23-905

Introduction

Glaucoma is one of the major causes of irreversible blindness worldwide. As a major risk factor of glaucoma, increased intraocular pressure (IOP) is leading to structural damage of the optic nerve and to visual field loss. An impaired or blocked drainage of aqueous humour via the trabecular meshwork in the chamber angle (CA) is a common reason for an increased IOP. In open angle glaucoma, the control of aqueous humour drainage is the central treatment goal, which can be achieved by pharmacological therapy or surgical procedures, e.g., by trabeculectomy, canaloplasty or minimally invasive glaucoma surgery (MIGS). With regard to MIGS, restoration of aqueous humour drainage by means of a small alloplastic implant represents a promising treatment option (1,2). The in-house developed Rostock glaucoma microstent (RGM) represents an innovational contribution in the therapy of glaucoma but is still in the phase of preclinical testing (3,4). The ongoing development of new (ophthalmological) implants demands critical evaluation and adjustment to reach a safe clinical use on the patient. In the preclinical trials, various evaluation steps are necessary. In advance, an appropriate animal model has to be chosen, on which the necessary preclinical *in vivo* trials will be conducted. The selected animal model should provide sufficient similarities in both anatomy and size to the human eye in which the implant is to be finally implanted. Under these premises, the surgical implantation process and the function of the implant can be adequately tested. Results of these *in vivo* trials themselves require evaluation, which, especially in the case of newly developed implants, depend on the correct placement within the tissue and favourable interactions with the surrounding tissue. In these phases of preclinical development, visualization by means of minimally invasive micro-computed tomography (micro-CT) offers considerable advantages for showing detailed positional relationships of the implant in the target organ.

The RGM is a valve-controlled and drug-eluting microstent for MIGS manufactured from a polycarbonate-based silicone elastomer. It measures 10 mm with an outer diameter of approximately 0.6 mm and an inner diameter of 0.3 mm. The drainage of the aqueous humour from the anterior chamber is regulated by means of a micromechanical valve (3). A drug-eluting coating (covering a length of 6 mm of the outflow area) is aiming for an antifibrotic positioning between the ocular tissues (5). The coating contains pirfenidone as antifibrotic agent to ensure long-term functionality of the microstent and bleb (6,7). The outflow is draining either suprachoroidally or subconjunctivally into the Tenon space.

In preclinical ophthalmological research, pigs and rabbits represent the preferred animal models. In the development of glaucoma stents, the morphology and size of the anterior chamber, morphometries of cornea and iris as well as the size of the entire eye play important roles in order to achieve implantation results comparable to those in humans. The human eye has a mean size of approximately 24 mm in anteroposterior extension and 23.5 mm in horizontal extension (8,9). In comparison, the size of the porcine eye is similar with 23.9 mm (anteroposterior) and 25.5 mm (horizontal) (10). The rabbit eye, however, differs in sizes and measures 16–19 mm in anteroposterior and 18–20 mm in horizontal direction (8). Nonetheless, the depth of the anterior chamber of the rabbit eye [2.9 mm (8)] resembles the human eye [3.5 mm (8)] rather than does the porcine eye [2.5 mm (10)]. According to the dimensions of the implant (RGM) to be tested, an appropriate animal model needs to be carefully selected which requires appropriate evaluation in advance.

Micro-CT is a valuable method for the detailed anatomical investigation of ocular soft tissues (11,12). As demonstrated in previous studies (13-16), micro-CT enables detailed, 3-dimensional (3D) imaging of the entire eye without a decrease in the visualization quality of internal structures as seen in sonography or optical coherence tomography. Detailed scanning with micro-CT provides imaging with high resolution below 100 µm and can be advanced to single-digit µm values which approximates light microscopy (13,16). For scans under moist conditions, best contrasting results of soft tissues are achieved with aqueous Lugol's iodine which allows differentiation of a variety of ocular tissues in the anterior eye region (11,12). In addition, micro-CT is characterized by the absence of structural damage and artificial alterations, such as those caused by histological processing (17)

which becomes problematic when investigating alloplastic implants after implantation (14).

An adequate positioning in the targeted tissue regions is essential for the performance of our in-house developed RGM with its valve-controlled inflow and a drug-eluting portion. Considering differences in ocular dimensions and morphology to the human eye, the aim of this study is to evaluate the applicability of two animal models for proper implantation of our developed RGM in the preclinical phase.

Methods

Samples

Porcine eyes (n=2; female) were obtained from mature German Landrace pigs (*Sus scrofa domesticus* Erxleben, 1777) provided by the Research Institute for Farm Animal Biology (FBN) in Dummerstorf, Germany. The samples were slaughter products that would otherwise have been disposed of—therefore no relevant approvals were required.

Rabbit eyes (n=2; female) were obtained from mature New Zealand White rabbits (*Oryctolagus cuniculus* Linnaeus 1758). The rabbits were commercially provided by Charles River Laboratories. The samples were taken under good laboratory practice (GLP)-conditions. The *in vivo* trials on rabbits were approved by the governmental ethical board for animal research [State Department of Agriculture, Food Security and Fisheries Mecklenburg-Western Pomerania (LALLF M-V)] under ethics number 7221.3-1-005/18 and carried out in accordance with the German Animal Welfare Law and the EU-directive 2010/63.

Human eyes were obtained from body donations (n=2; female and male) at the Institute of Anatomy (Rostock University Medical Center) which was approved by the Rostock University Medical Center ethics committee (approval ID: A2014-0100). Body donors gave their informed consent during lifetime to use their remains for research studies. The study was conducted in accordance with the Declaration of Helsinki (as revised in 2013).

After orbital exenterations, a RGM was surgically placed in the anterior chamber draining in the subconjunctival space. The conjunctiva was opened close to the eye limbus and a subconjunctival pouch was formed towards the posterior eye pole. With a 1.3 mm paracentesis lancet (#LP7594, Bausch + Lomb GmbH, Berlin, Germany) a passage through the sclera was formed close to limbus to the anterior chamber. The outstream region of the microstent was placed in the subconjunctival pouch and sutured (7-0 vicryl, #QCMCPQ, Ethicon, New Jersey, USA).

The ocular globes with implanted RGM were initially fixated by immersion in 3.7% buffered formaldehyde which was exchanged after one day. During fixation, samples were placed on a shaker (60 rpm) up to one week at room temperature (RT). After fixation, samples were washed by immersion in phosphate-buffered saline for up to 24 hours at RT.

Tissue contrasting

Samples were transferred to 75 mL 1% Lugol's iodine (Carl Roth GmbH + Co. KG, Karlsruhe, Germany) and stored for at least two weeks on a shaker (60 rpm) at RT. The contrast agent was exchanged 2–3 times until no decolouration (agent depletion) was noticed (11).

Prior to the micro-CT scan, samples were washed in distilled water for 0.5 to 2 hours to remove residuals of the contrasting agents.

Micro-CT

Samples were mounted in centrifuge tubes filled with fresh distilled water for micro-CT scanning. Virtual image stacks were obtained with a Xradia Versa 410 X-ray microscope (Carl Zeiss Microscopy GmbH, Jena, Germany). Micro-CT scans of the ocular samples were done at 60 kV and 133 mA (8 W) with a 0.4× objective, the single non-implanted RGM at 40 kV and 200 mA (8 W) with a 4× objective in vertical stitch mode using the software Scout and Scan v.11.1 (Carl Zeiss Microscopy GmbH). Detailed scan parameters for each sample are listed in *Table 1*.

Samples were positioned close to the X-ray source for maximum geometric magnification. The field of view was chosen to encompass the whole diameter of the ocular bulb.

3D reconstruction and image processing

Volume rendering of the micro-CT-based image stacks, 3D reconstructions and virtual sections were created with the software Imaris (8.4, Bitplane, Switzerland). Measurements of the eyes and of the implanted microstents were performed using the "Measurement Points" tool in the software Imaris (*Figure 1*). The number (n) of measurement points for each parameter (*Table 2*) per specimen (2 per species) was at:

❖ Globe length (GL): n=1;

Table 1 Parameters applied for conducted micro-CT scans

Sample	Exposure time (seconds)	Sample rotation (°)	Projection increment (°)	Filter (physical)	Voxel size (µm)	Figures
Rostock glaucoma microstent	6	360	0.36	LE1†	1.8	2
Rabbit eye						
Sample 1	7	220	0.275	LE6†	20.5	3A,3B,3D
Sample 2	7	220	0.275	LE6†	20.5	3C
Porcine eye						
Sample 1	10	216	0.24	LE5†	19.0	4
Sample 2	10	216	0.24	LE5†	19.0	Not shown
Human eye						
Sample 1	15	220	0.244	LE6†	30.8	5A-5C
Sample 2	8	222	0.247	LE6†	27.8	5D

†, ZEISS developed and protected. Micro-CT, micro-computed tomography.

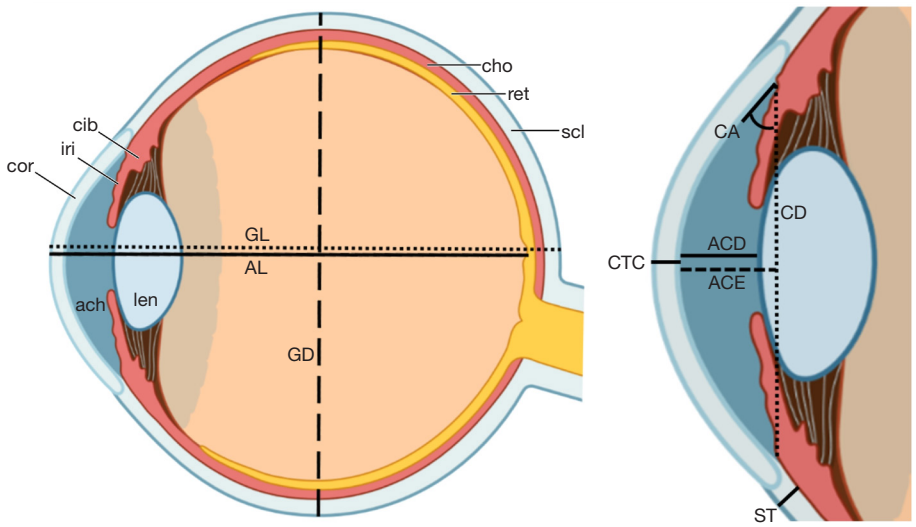

Figure 1 Schematic drawing of the eye illustrating the measured parameter given in *Table 2*. Created with BioRender.com. ACD, anterior chamber depth; ACE, anterior chamber depth (extended to CD); AL, axis length; CA, chamber angle; CD, chamber diameter; CTC, corneal thickness (central); GD, globe diameter; GL, globe length; ST, sclera thickness (postlimbal); ach, anterior chamber; cho, choroidea; cib, ciliary body; cor, cornea; iri, iris; len, lens; ret, retina; scl, sclera.

- ❖ Axis length (AL): n=1;
- ❖ Globe diameter (GD): n=2;
- ❖ Cornea thickness (central) (CTC): n=1;
- ❖ Anterior chamber depth (extended to chamber diameter) (ACE): n=2;
- ❖ Anterior chamber depth (ACD): n=1;
- ❖ Chamber diameter (CD): n=2;
- ❖ CA: n=4;
- ❖ Sclera thickness (postlimbal) (ST): n=4.

Based on the technical parameters of the RGM (18), the stents were measured based on micro-CT scans to differentiate between the area with and without drug-eluting coating. The areas were segmented and color-masked accordingly (see *Figure 2*).

Table 2 Ocular dimensions in rabbit, porcine and human eye samples obtained from micro-CT based measurements

Parameters	Rabbit eye	Porcine eye	Human eye
Globe length (mm)	13.4–15.5 (14.45±1.05)	16.80–16.80 (16.80±0)	24.8–25.1 (24.95±0.15)
Axis length (mm)	12.8–14.8 (13.8±1.00)	15.2–15.5 (15.35±0.15)	23.7–24.5 (24.1±0.40)
Globe diameter (mm)	15.5–18 (16.65±0.94)	21.6–24.1 (22.95±0.90)	24.4–26.6 (25.48±0.87)
Cornea thickness, central (mm)	0.29–0.31 (0.30±0.01)	0.90–1.08 (0.99±0.09)	0.41–0.73 (0.57±0.16)
Anterior chamber depth, extended (mm)	4.05–5.06 (4.56±0.36)	2.31–2.96 (2.60±0.24)	1.53–3.42 (2.75±0.86)
Anterior chamber depth (mm)	2.45–3.18 (2.82±0.36)	1.40–1.83 (1.62±0.22)	–
Chamber diameter (mm)	11.4–13.4 (12.58±0.83)	12.4–14.3 (13.33±0.68)	11.8–12.6 (12.23±0.33)
Chamber angle (°)	53.9–83.9 (65.58±8.82)	23.8–36.3 (32.01±4.16)	33.5–56.1 (45.48±7.29)
Sclera thickness, postlimbal (mm)	0.38–0.57 (0.46±0.07)	0.88–1.52 (1.23±0.26)	0.37–0.56 (0.49±0.05)

Data are presented as range (mean ± standard deviation). "–" denotes no values available due to intraocular lens implant or dislocated lens. For clearer understanding, parameters are visualized in *Figure 1*. Micro-CT, micro-computed tomography.

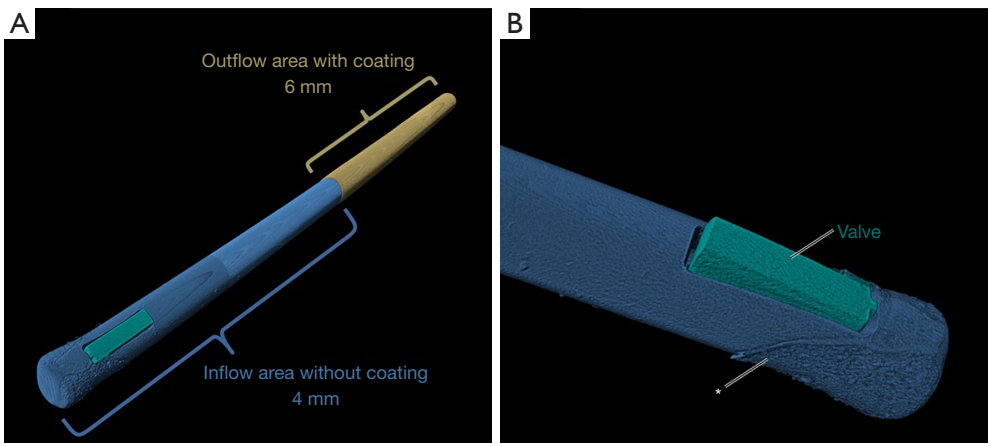

Figure 2 Micro-CT scan of Rostock Glaucoma Microstent, volume rendering with artificial masking depicting inflow (blue) with the valve (cyan) and outflow (yellow) areas. (A) Perspective overview on the Rostock Glaucoma Microstent with measurements on the distinct areas. (B) Detail on inflow area with valve-mechanism (cyan). *, roughened surface and fringe are visualization artefacts caused by sample holder. Micro-CT, micro-computed tomography.

The figure plates were arranged using CorelDRAW Graphics Suite 2017 (Corel Corporation, Ottawa, ON, USA). Images were embedded into CorelDRAW 2017 files and edited in Corel PHOTO-PAINT 2017 using general imaging enhancement tools (contrast, brightness).

Results

RGM in rabbit eye

The rabbit eyes (New Zealand White) had a size of 13.4–15.5 mm in the anteroposterior extension and a diameter of 15.5–18 mm (*Table 2*). These dimensions provided sufficient space to place the RGM which had a total length of 10 mm (*Figure 3A-3C*). In the anterior segment of the eye, the cornea stretched with a thickness of 0.3 mm in the central region. Posterior to the cornea, the anterior chamber extended with a depth of 2.45–3.18 mm (*Figure 3C*). The diameter of the anterior chamber measured 11.4–13.4 mm between the opposite CAs, in which the inflow area of the microstent with a length of 4 mm was placed (*Figure 3A-3C*). The CA was measured with a range of 53.9°–83.9° in the rabbit eye (*Figure 3C*). The passage of

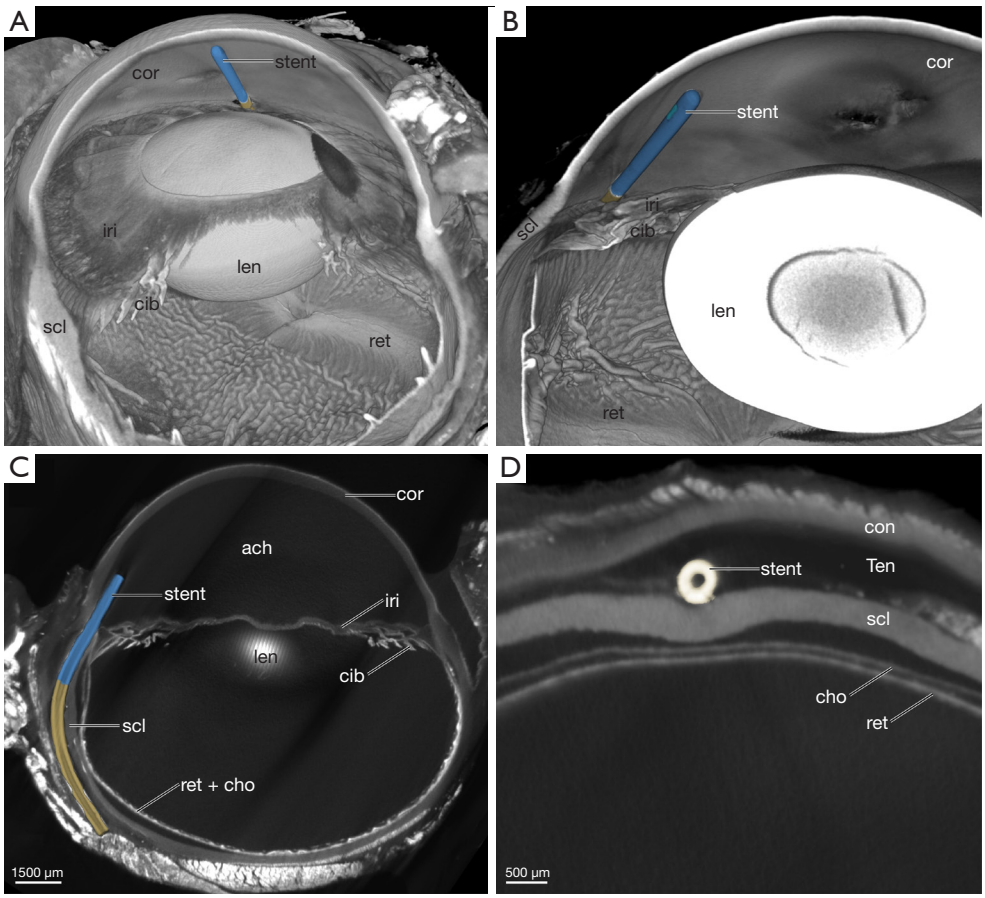

Figure 3 Micro-CT scans of rabbit eye with implanted Rostock Glaucoma Microstent, artificial colour masking of microstent areas. (A,B) Volume rendering showing position of Rostock Glaucoma Microstent in the anterior chamber: (A) clipping plane through anterior and posterior chamber in antero-dorsal view; (B) clipping plane through anterior chamber, enlarged view in antero-ventral view. (C) Virtual section to rabbit eye longitudinally through Rostock Glaucoma Microstent showing its lumen. (D) Virtual frontal section showing the position of the outflow area within Tenon space. cor, cornea; iri, iris; scl, sclera; cib, ciliary body; len, lens; ret, retina; stent, Rostock Glaucoma Microstent; ach, anterior chamber; cho, choroidea; con, conjunctiva; Ten, Tenon space; micro-CT, micro-computed tomography.

the microstent into the CA was realized via the sclera in the postlimbal region (*Figure 3C*). The scleral thickness at this location ranged from 0.38–0.57 mm. The outflow area of the RGM had a length of 6 mm and was placed subconjunctivally in the Tenon space (*Figure 3C,3D*). The RGM extended well into the posterior region of the rabbit eye, where it was partially flanked by the extraocular muscles (*Figure 3C,3D*).

RGM in porcine eye

The dimensions of the porcine eye (German Landrace) were larger than in the rabbit eye with an anteroposterior length of 16.8 mm and a diameter of 21.6–24.1 mm (*Table 2*). So, the RGM could be adequately placed (*Figure 4A-4C*). The cornea appeared three times thicker than in the rabbit eyes (0.90–1.08 mm). But with regard to the depth of the anterior chamber (1.40–1.83 mm) and to CA (23.8°–36.3°), the porcine eyes had smaller values than rabbit eyes (*Table 2*, *Figure 4C*). As a result, there is little space between cornea and iris in the anterior chamber to place the RGM (*Figure 4B,4C*). The diameter of the anterior chamber measured between 12.4–14.3 mm and was large enough to place the inflow area of the RGM (*Figure 4A-4C*). The incision for the RGM was made through a sclera with thickness of 0.88–1.52 mm, which was more than twice as much as in rabbits. The outflow area of the RGM was placed subconjunctivally in the Tenon space (*Figure 4B-4D*).

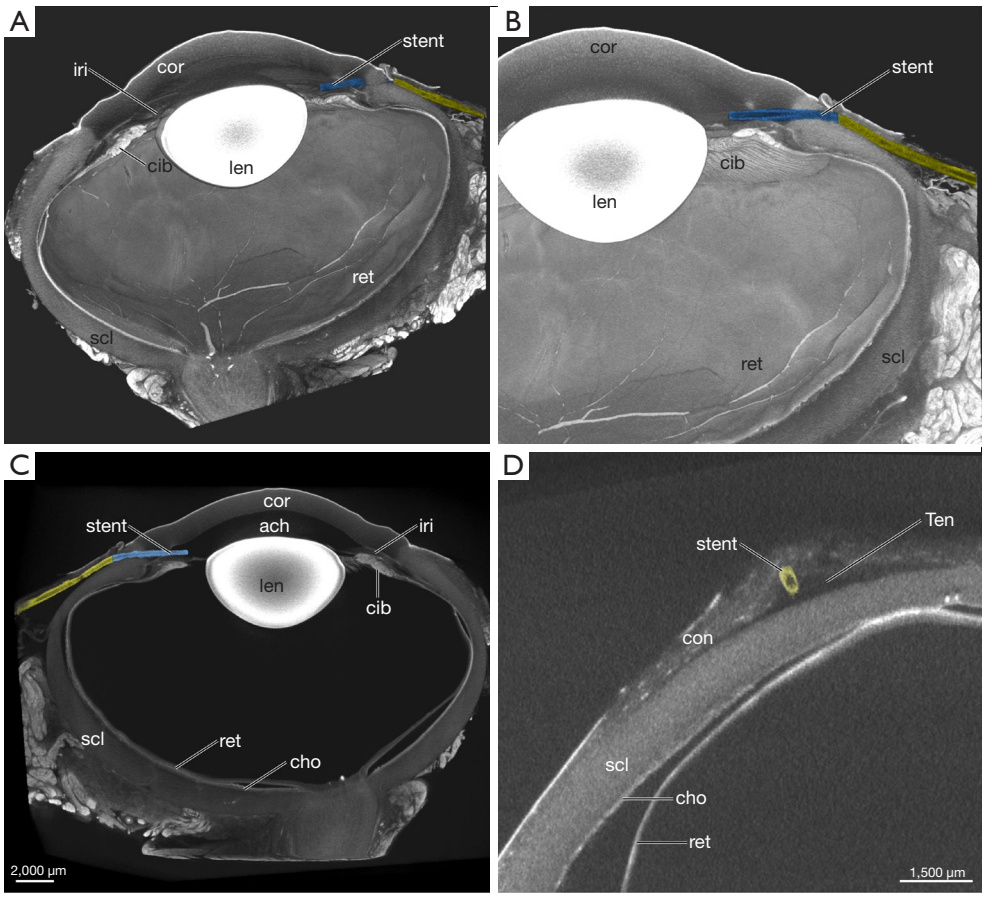

Figure 4 Micro-CT scans of porcine eye with implanted Rostock Glaucoma Microstent, artificial colour masking of microstent areas. (A,B) Volume rendering showing position of Rostock Glaucoma Microstent in the anterior chamber: (A) clipping plane through anterior and posterior chamber in ventro-lateral view; (B) clipping plane through anterior chamber, enlarged view in ventro-lateral view. (C) Virtual section to porcine eye longitudinally through Rostock Glaucoma Microstent showing its lumen. (D) Virtual frontal section showing the position of the outflow area within Tenon space. cor, cornea; iri, iris; cib, ciliary body; len, lens; ret, retina; scl, sclera; stent, Rostock Glaucoma Microstent; ach, anterior chamber; cho, choroidea; con, conjunctiva; Ten, Tenon space; micro-CT, micro-computed tomography.

Here, the RGM remained in the anterior half of the eye globe only covered by the conjunctiva anterior to the extraocular muscles (*Figure 4C,4D*).

RGM in human eye

In comparison to the animal models, the size of the human eye was more similar to the porcine eye with a GL of 24.8–25.1 mm and a diameter of 24.4–26.6 mm (*Table 2*). The central thickness of the cornea ranged from 0.41 to 0.73 mm in the samples and was between the values of porcine and rabbit eyes. Due to dislocated lens and intraocular lens (IOL) implants, the values for the depth of the anterior chamber (distance between posterior corneal endothelium and lens) could not be obtained. Alternatively, the distance between posterior corneal endothelium and the virtual line connecting the opposite CAs was taken (ACE, *Figure 1*) with a distance of 1.53–3.42 mm. Corresponding comparative values were also measured in the rabbit and porcine eyes and are given in *Table 2*. The diameter of the anterior chamber measured 11.8–12.6 mm between the opposite CAs (*Figure 5A-5C*). The RGM was placed in the CA, which opens with a range of 33.5°–56.1° (*Figure 5C*). Comparable to the condition in porcine eyes, the human eye also provided enough space in the anterior chamber to place the RGM. Concerning the scleral thickness, the

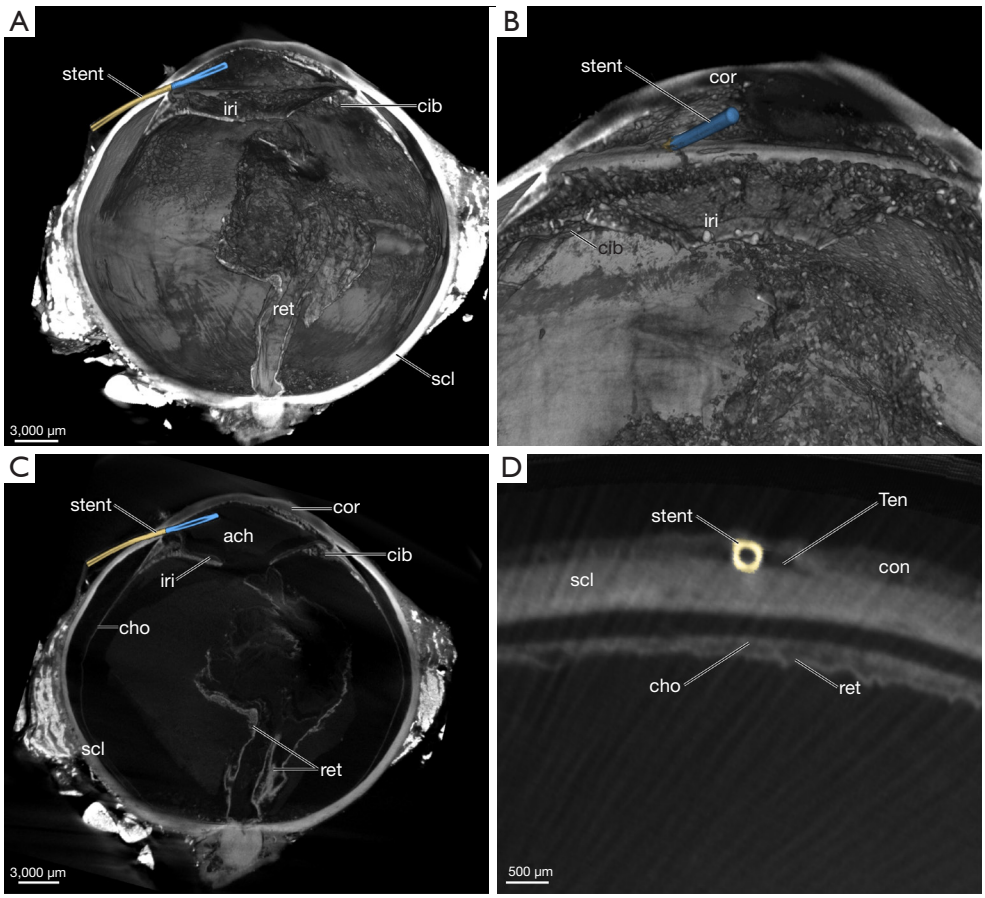

Figure 5 Micro-CT scans of human eye with implanted Rostock Glaucoma Microstent, artificial colour masking of microstent areas—note the extensively detached retina (A-C). (A,B) Volume rendering showing position of Rostock Glaucoma Microstent in the anterior chamber: (A) clipping plane through anterior and posterior chamber in dorsal view; (B) clipping plane through anterior chamber, enlarged view in dorsal view. (C) Virtual section to human eye longitudinally through Rostock Glaucoma Microstent showing its lumen. (D) Virtual frontal section showing the position of the outflow area within Tenon space. stent, Rostock Glaucoma Microstent; iri, iris; cib, ciliary body; ret, retina; scl, sclera; cor, cornea; ach, anterior chamber; cho, choroidea; ach, anterior chamber; con, conjunctiva; Ten, Tenon space; micro-CT, micro-computed tomography.

condition of the human eye resembled the rabbit sclera with sufficient 0.37–0.56 mm to insert the RGM (*Figure 5C*). The outflow area of the RGM was placed subconjunctivally in the Tenon space (*Figure 5C,5D*). Likewise, as in porcine eyes, the RGM remained in the anterior half of the eye globe where it was covered by the conjunctiva anterior to the extraocular muscles (*Figure 5C,5D*).

Discussion

Microstent implantation in human and animal model eyes

When searching for an appropriate animal model for implantation and functional trials of newly developed glaucoma microstent and implants in general, micro-CT imaging provides valuable analytic capabilities. In particular, the digital measurement tools enable in-depth analysis to relate the dimensions of the eyes of different organisms to the implanted glaucoma microstent. This is of particular importance for application-oriented studies of implant development when measures are not available (in the literature). Besides the measurement, micro-CT enables detailed visualization of the implant within the yielded position and therefore a qualitative evaluation of the implantation result.

The measured dimensions for rabbit and porcine eye

differed from the reference data given in the literature. Rabbit eyes in our study were slightly smaller compared to data in the literature, in both GL and diameter which is 16–19 mm and 17–18 mm, respectively (8,19,20). Differences to the literature were more pronounced for the porcine eyes, which are reported with 23.9 mm in GL extension and 24.5–25.5 mm in diameter (10). The dimensions of the human eyes were within a range of published values (8-10,19,21). Discrepancies in the animal model can be attributed to different animal breeds and different ages of the individuals, for which information are not always evident.

Tissue damages are mainly caused by storage conditions prior to obtainment of the specimens [see (11)]. In the relevant structures of the anterior chamber of the eye, the collapsed cornea in porcine and human specimens as well as damaged lens in the human specimens were obviously artefacts present prior to the stent application (11). Dislocated lenses or implanted IOL compromised the comparability of the ACD measurements with the animal models used. For better comparability, the distance between the cornea and the line connecting the opposite CAs was therefore measured in addition (see ACE in *Figure 1*).

Based on the morphometric parameters, the porcine eye corresponds most closely to the human eye in terms of globe size and most ocular structures (see *Table 2*). Merely, central corneal thickness, postlimbal scleral thickness, and anterior CD of the rabbit are more similar to the human eye. Yet, despite the better morphological correlation between human and porcine eye, the *ex vivo* implantation experiments in the rabbit yielded highly satisfactory results for the implant, too. In particular, the similar thickness of the sclera in the postlimbal region in rabbits allows an optimal replication of the surgical procedure in humans (*Table 2*). Measurements of the sclera in the postlimbal region are rare in the literature [0.138 mm in rabbit (20), 1.34 mm in porcine (22), 0.564 mm in human (22)] and differ considerably from the values in this study (*Table 2*). With respect to the here presented data, the scleral thickness of rabbit (0.38 mm) and human eyes (0.37 mm) is considerably concordant. It can be expected that the pressure of the sclera on the inserted silicone microstent is also comparable and deformations of the stent cross-section might therefore better simulated than in porcine eyes. The larger CA and the deeper anterior chamber in rabbits compared to pigs facilitate an appropriate placement of the inflow area of the RGM in the anterior chamber and reduce the risk of injury to adjacent structures (*Table 2*) (19,21,22). The placement of the outflow area of the microstent in the subconjunctival space (Tènon space) could be ensured in both animal models to realize aqueous humour drainage. However, in the rabbit, the microstent might project far into the posterior region of the eye, which is not the case in the pig.

Overall, the implantation results in pigs and humans are more comparable with respect to the overall size ratio with a flatter stent position inside the anterior chamber and a weaker bending towards the placement of the outflow area under the anterior conjunctiva. On the other hand, the rabbit eye with its spacious anterior chamber provides conditions for a successful and low-risk implantation while ensuring the functionality of the RGM. In particular, with regard to the scleral thickness, which directly interacts with the flexible stent, the human conditions are better represented in the rabbit eye. In addition, rabbits are cost effective, easy to rear and to prepare for surgical operations which favour their use in preclinical *in vivo* studies. However, with regard to the optimization of implantation techniques and surgical training and their risk assessment, the porcine eye is the model of choice for the RGM.

Micro-CT implementation into in vivo studies

The value of micro-CT imaging becomes evident for morphological *ex vivo* analyses. A targeted integration into preclinical *in vivo* studies, in which properties, functionality of alloplastic implants and tissue reactions are tested, allows a more differentiated interpretation of measured values and diagnostical data. The final step in an animal experiment is generally the euthanasia of the test animals, which should be followed by sampling the target organ for subsequent micro-CT imaging. Spatial high-resolution scans provide detailed insights into the condition of the implant and can reveal unintended deformations, damages or material changes subsequent to the experiment to infer on the functionality of the implant. In the case of the RGM, information about the aimed implant placement and possible implant stenosis or blockages of the valve was provided (*Figure 2B*). On the other side, tissue reactions to alloplastic materials can be assessed, too. These potentially include, changes in tissue structure, fibrotic reactions, tissue growth or damage and scarring that may occur as a result of the surgical procedure and as a reaction in the implant material. For this purposes, micro-CT provides valuable advantages as it is a non-destructive method with regard to sample preparation and imaging with which structures deeply located within tissues can be visualized (11). In

contrast, classical imaging methods of similar resolution as bright field microscopy-based histology strongly interfere with the sample and can cause alterations like sectioning artefacts (17). Especially, the displacement of tissue fragments from the lumen of stents is a limiting factor for the use of histological sections to interpret its functionality in aimed position (17).

Limitations in the application of micro-CT imaging exist in the examination of metallic implants, which can cause beam-hardening effects as imaging artefacts in the surrounding. On the other hand, beam-hardening may be reduced by using X-ray beam filters (23), software solutions [e.g., (24)] or sample preparation such as enhancing the X-ray attenuation [see (25)].

Micro-CT studies could thus contribute to the interpretation of results from *in vivo* studies and promote the development of novel implant techniques. Moreover, the evaluation of implantation results by micro-CT can also contribute to improve animal welfare in the context of animal experimentation concerning the 3Rs principle (replacement, reduction, refinement). Subsequent to the *in vivo* experiment, organs that are further utilized for micro-CT based visualization reduce the use of experimental animals (and prototypes of implants), as redundant implantations for imaging purposes can be partially omitted. The *a posteriori* evaluation of performed surgical interventions can be directly used to make adjustments and improvements of the procedure in subsequent implantation trials, and thus make an important contribution in terms of refinement.

Conclusions

In conclusion, micro-CT has proven to be a valuable tool for postoperative evaluation of implanted glaucoma drainage devices (*ex vivo*) in its entire complexity. Compared to the human eye, the porcine eye is the ideal choice to optimize implantation techniques and surgical training of subconjunctivally draining glaucoma stents due to correspondences in size ratios and morphology. The rabbit eye morphology, however, facilitates more effective microstent implantation and provides all prerequisites to ensure the functionality of the implant comparable to the human eye. Moreover, the economic keeping conditions (e.g., less space required, shorter breeding periods) and the requisition during surgical procedure, make the rabbit the ideal model for preclinical *in vivo* trials for the ongoing evaluations of the RGM.

The targeted implementation of micro-CT scans aids the interpretation of preclinical animal studies, offers new approaches for the development of alloplastic implants and can contribute to the improvement of animal experimentation in the context of the 3Rs principle.

Acknowledgments

We are grateful to the Research Institute for Farm Animal Biology (FBN) in Dummerstorf for providing enucleated porcine eyes for our studies. Stephan Scholz is thanked for his technical support. Laura Hiepe is thanked for her help with enucleating eyes from human body donations. Parts of the results were presented as a poster contribution at the annual congress of the German Ophthalmological Society (DOG) 2022 in Berlin. We would like to thank the German Ophthalmological Society (DOG) and Springer Publisher for the exemption from the publication obligation and the waiver of copyrights.

Funding: This work was supported by the German Federal Ministry of Education and Research (grant No. FKZ 03ZZ0931A). The micro-CTs used in this study were jointly sponsored by the German Research Foundation (DFG) and the Federal State Mecklenburg-Western Pomerania (grant No. DFG INST 264/130-1 FUGG). We acknowledge the financial support by Deutsche Forschungsgemeinschaft and Universität Rostock/Universitätsmedizin Rostock within the Open Access Publishing funding program.

Footnote

Conflicts of Interest: All authors have completed the ICMJE uniform disclosure form (available at https://qims.amegroups.com/article/view/10.21037/qims-23-905/coif). The authors have no conflicts of interest to declare.

Ethical Statement: The authors are accountable for all aspects of the work in ensuring that questions related to the accuracy or integrity of any part of the work are appropriately investigated and resolved. The study was conducted in accordance with the Declaration of Helsinki (as revised in 2013) and approved by the Rostock University Medical Center ethics committee (approval ID: A2014-0100). Body donors gave their informed consent during lifetime to use their remains for research studies. The *in vivo* trials on rabbits were approved by the governmental ethics board for animal research [State Department of Agriculture, Food Security and Fisheries Mecklenburg-

Western Pomerania (LALLF M-V)] under ethical number 7221.3-1-005/18 and carried out in accordance with the German Animal Welfare Law and the EU-directive 2010/63.

References

1. Lee DA, Higginbotham EJ. Glaucoma and its treatment: a review. Am J Health Syst Pharm 2005;62:691-9.
2. Lavia C, Dallorto L, Maule M, Ceccarelli M, Fea AM. Minimally-invasive glaucoma surgeries (MIGS) for open angle glaucoma: A systematic review and meta-analysis. PLoS One 2017;12:e0183142.
3. Siewert S, Schmidt W, Kaule S, Kohse S, Stiehm M, Kopp F, Stahnke T, Guthoff R, Grabow N, Schmitz KP. Development of a microstent system for minimally invasive glaucoma surgery. Curr Dir Biomed Eng 2017;3:779-81.
4. Siewert S, Kischkel S, Brietzke A, et al. Development of a Novel Valve-Controlled Drug-Elutable Microstent for Microinvasive Glaucoma Surgery: In Vitro and Preclinical In Vivo Studies. Transl Vis Sci Technol 2023;12:4.
5. Siewert S, Pfensig S, Großmann S, Stiehm M, Schmitz KP, Schmidt W, Kohse S, Wulf K, Grabow N, Kopp F, Guthoff R. Development of a drug-eluting microstent for micro-invasive glaucoma surgery. Curr Dir Biomed Eng 2018;4:603-6.
6. Stahnke T, Kowtharapu BS, Stachs O, Schmitz KP, Wurm J, Wree A, Guthoff RF, Hovakimyan M. Suppression of TGF-β pathway by pirfenidone decreases extracellular matrix deposition in ocular fibroblasts in vitro. PLoS One 2017;12:e0172592.
7. Stahnke T, Siewert S, Reske T, Schmidt W, Schmitz KP, Grabow N, Guthoff RF, Wree A. Development of a biodegradable antifibrotic local drug delivery system for glaucoma microstents. Biosci Rep 2018;38:BSR20180628.
8. Gwon A. The rabbit in cataract/IOL surgery. In: Panagiotis AT. editor. Animal Models in Eye Research. London: Academic Press 2008; 184-204.
9. Augusteyn RC, Nankivil D, Mohamed A, Maceo B, Pierre F, Parel JM. Human ocular biometry. Exp Eye Res 2012;102:70-5.
10. Sanchez I, Martin R, Ussa F, Fernandez-Bueno I. The parameters of the porcine eyeball. Graefes Arch Clin Exp Ophthalmol 2011;249:475-82.
11. Runge J, Stahnke T, Guthoff RF, Wree A, Keiler J. Micro-CT in ophthalmology: ex vivo preparation and contrasting methods for detailed 3D-visualization of eye anatomy with special emphasis on critical point drying. Quant Imaging Med Surg 2022;12:4361-76.
12. Keiler J, Stahnke T, Guthoff RF, Wree A, Runge J. Ex Vivo Micro-CT in Ophthalmology: Preparation and Contrasting for Non-invasive 3D-Visualisation. Klin Monbl Augenheilkd 2023;240:1359-68.
13. Hann CR, Bentley MD, Vercnocke A, Ritman EL, Fautsch MP. Imaging the aqueous humor outflow pathway in human eyes by three-dimensional micro-computed tomography (3D micro-CT). Exp Eye Res 2011;92:104-11.
14. Enders C, Braig EM, Scherer K, Werner JU, Lang GK, Lang GE, Pfeiffer F, Noël P, Rummeny E, Herzen J. Advanced Non-Destructive Ocular Visualization Methods by Improved X-Ray Imaging Techniques. PLoS One 2017;12:e0170633.
15. Leszczyński B, Sojka-Leszczyńska P, Wojtysiak D, Wróbel A, Pędrys R. Visualization of porcine eye anatomy by X-ray microtomography. Exp Eye Res 2018;167:51-5.
16. Tkachev SY, Mitrin BI, Karnaukhov NS, Sadyrin EV, Voloshin MV, Maksimov AY, Goncharova AS, Lukbanova EA, Zaikina EV, Volkova AV, Khodakova DV, Mindar MV, Yengibarian MA, Protasova TP, Kit SO, Ermakov AM, Chapek SV, Tkacheva MS. Visualization of different anatomical parts of the enucleated human eye using X-ray micro-CT imaging. Exp Eye Res 2021;203:108394.
17. Stahnke T, Hadlich S, Wree A, Guthoff RF, Stachs O, Langner S. Magnetic Resonance Microscopy of the Accommodative Apparatus. Klin Monbl Augenheilkd 2016;233:1320-3.
18. Siewert S, Reske T, Pfensig S, Großmann S, Stiehm M, Schmitz KP, Schmidt W, Grabow N, Stahnke T, Guthoff R. Development of an antifibrotic drug-eluting coating for a minimally invasive implantable glaucoma microstent. Curr Dir Biomed Eng 2019;5:215-8.
19. Uthoff D. Biometric studies on the rabbit eye. Klin Monbl Augenheilkd 1984;185:189-92.
20. Barathi A, Thu MK, Beuerman RW. Dimensional growth of the rabbit eye. Cells Tissues Organs 2002;171:276-85.
21. Langner S, Martin H, Terwee T, Koopmans SA, Krüger PC, Hosten N, Schmitz KP, Guthoff RF, Stachs O. 7.1

T MRI to assess the anterior segment of the eye. Invest Ophthalmol Vis Sci 2010;51:6575-81.
22. Menduni F, Davies LN, Madrid-Costa D, Fratini A, Wolffsohn JS. Characterisation of the porcine eyeball as an in-vitro model for dry eye. Cont Lens Anterior Eye 2018;41:13-7.
23. Meganck JA, Kozloff KM, Thornton MM, Broski SM, Goldstein SA. Beam hardening artifacts in micro-computed tomography scanning can be reduced by X-ray beam filtration and the resulting images can be used to accurately measure BMD. Bone 2009;45:1104-16.
24. Verburg JM, Seco J. CT metal artifact reduction method correcting for beam hardening and missing projections. Phys Med Biol 2012;57:2803-18.
25. Koç MM, Aslan N, Kao AP, Barber AH. Evaluation of X-ray tomography contrast agents: A review of production, protocols, and biological applications. Microsc Res Tech 2019;82:812-48.

Cite this article as: Runge J, Kischkel S, Keiler J, Grabow N, Schmitz KP, Siewert S, Wree A, Guthoff RF, Stahnke T. Experimental glaucoma microstent implantation in two animal models and human donor eyes—an *ex vivo* micro-computed tomography-based evaluation of applicability. Quant Imaging Med Surg 2024;14(8):5321-5332. doi: 10.21037/qims-23-905

